Table 1. Prostaglandin production (pg/mg total protein) in the ischemic hemisphere

Prostaglandin	Duration of ischemia	Peri-infarct area	Ischemic core
PG E_2	0 hours	60.8 ± 16.6	21.4 ± 11.4
	3 hours	156.6 ± 70.1	54.4 ± 22.3
	24 hours	2,609.0 ± 2,522.0 *†	414.6 ± 226.3 *†
Prostacyclin metabolite (6-keto-PG $F_{1\alpha}$)	0 hours	122.3 ± 47.6	47.6 ± 23.0
	3 hours	200.8 ± 59.7	93.4 ± 43.5
	24 hours	1,143.0 ± 623.7 *†	341.6 ± 84.5 *†

* $p < 0.05$ vs. 0 h (control) ; † : $p < 0.05$ vs. 3 h ischemia by ANOVA
The values were the mean ± SD.

Significant reductions in CBF in the peri-infarct areas and ischemic core were demonstrated in animals at each ischemic time point compared to the controls (Fig. 1). The expression ratios of COX-2 mRNA increased significantly between 3 and 24 h of ischemia in the peri-infarct areas compared to the controls. In the ischemic core, significant increases in COX-2 mRNA were seen following 6 h of ischemia, which remained through 24 h. The peak value of the expression ratio of COX-2 protein in the peri-infarct area was 10.7 at 24 h of ischemia, while the peak expression ratio in the ischemic core was 2.0 at 6 h of ischemia. COX-2 immunoreactive neurons were found predominantly in the peri-infarct area. Elevations in the immunohistochemical staining of discrete neuronal populations were also observed in the ischemic core. Although no significant increases in PGE_2 and prostacyclin levels were observed in the peri-infarct and ischemic core areas following 3 h of ischemia, significant increases in prostaglandin levels were found in the ischemic hemisphere following 24 h of ischemia. In particular, PGE_2 levels in the peri-infarct area increased significantly (Table 1).

4. Discussion

The CBF pattern obtained in the SD model of primates differed from those obtained in other studies using rat- and cat-SD models[13,14]. The focal hyperemia was not followed by prolonged hypoperfusion. The changes in CBF during SD phenomenon in primates also differed from those in patients with migraine[15]. In biochemical analysis for brain tissues, COX-2 was induced in the cortices where SD was recorded, being in accord with prvious observations in rodent models[5].

We observed COX-2 expression during focal brain ischemia in a primate thromboembolic stroke model. In the ischemic core, in which a signficnat decrease in CBF were accompanied by reduced CMRglc, upregurated COX-2 mRNA at 2 h-ischemia but decreased by 24 h. Disappearance of COX-2 at 24 h-ischemia was parallel to a housekeeping GAPDH-mRNA reduction, indicating that ischemic injury was already apparent at 24-ischemia in the temporal cortex and the basal ganglia. In the peri-infarct area, on the contrary, induced expression of COX-2 mRNA was still found at 24-h ischemia in the parietal cortex with a mild CBF reduction and maintained CMRglc.

In the focal ischemia in rats, the time course of COX-2 expression in the ischemic core was different from that seen in the peri-infarct area. The upregulation of COX-2 mRNA in the peri-infarct area persisted for at least 24 h after ischemia, as did the production of COX-2 protein, which lead

to significant increases in prostacyclin as well as PGE_2 levels following 24 hours of ischemia, though significant increases in COX-2 mRNA persisted during the 24 h of ischemia, though significant increases in COX-2 protein were not observed. This latter finding may be attributable to the severe ischemic injury that was caused by reduced CBF, which likely affected protein synthesis[2]. In spite of these effects on COX-2 protein, significant increases were seen in the concentration of prostaglandins in the ischemic core 24 hours after ischemia. Local increases in neuronal COX-2 expression in the ischemic core, as determined by immunohistochemical analysis, could have accounted for this increase in prostaglandin concentration.

The induction of neuronal COX-2 is important for the regulation of prostaglandin signaling in post-ischemic regions, and the magnitude of COX-2 activity and prostaglandin production is determined by the degree and duration of CBF reduction. Before novel therapeutic options for stroke patients can be developed, further clarification of the effects of COX-2 during and after ischemia will be required.

Acknowledgment

This study was supported in part by a Grant-in-Aid for Scientific Research from the Japan Society for the Promotion of Science, by grants from the Takeda Medical Research Foundation, by the Mitsubishi Pharma Research Foundation, and by the Japan Heart Foundation.

References

1) Leao AAP : Spreading depression of activity in the cerebral cortex. J Neurophysiol 7 : 359—390, 1944
2) Hossmann KA : Viability thresholds and the penumbra of focal ischemia. Ann Neurol 36 : 557—565, 1994
3) Takano K, Latour LL, Formato JE, Carano RAD, Helmer KG, Hasegawa Y, Sotak CH, Fisher M : The role of spreading depression in focal ischemia evaluated by diffusion mapping. Ann Neurol 39 : 308—318, 1996
4) Stroke Therapy Academic Industry Roundtable : Recommendations for standards regarding preclinical neuroprotective and restorative drug development. Stroke 30 : 2752—2758, 1999
5) Miettinen S, Fusco FR, Yrjanheikki J, Keinanen R, Hirvonen T, Roivainen R, Narhi M, Hokfelt T, Koistinaho J : Spreading depression and focal brain ischemia induce cyclooxygenase-2 in cortical neurons through n-methyl-d-aspartic acid-receptors and phospholipase a_2. Proc Natl Acad Sci USA 94 : 6500—6505, 1997
6) Yokota C, Kuge Y, Hasegawa Y, Tagaya M, Abumiya T, Ejima N, Tamaki N, Yamaguchi T, Minematsu K : Unique profile of spreading depression in a primate model. J Cereb Blood Flow Metab 22 : 835—842, 2002
7) Yokota C, Inoue H, Kuge Y, Abumiya T, Tagaya M, Hasegawa Y, Ejima N, Tamaki N, Minematsu K : Cyclooxygenase-2 expression associated with spreading depression in a primate model. J Cereb Blood Flow Metab 23 : 395—398, 2003
8) Kito G, Nishimura A, Susumu T, Nagata R, Kuge Y, Yokota C, Minematsu K : Experimental thromboembolic stroke in cynomolgus monkey. J Neurosci Meth 105 : 45—53, 2001
9) Kuge Y, Yokota C, Tagaya M, Hasegawa Y, Nishimura A, Kito G, Tamaki N, Hashimoto N, Yamaguchi T, Minematsu K : Serial changes in cerebral blood flow and flow-metabolism uncoupling in primates with acute thromboembolic stroke. J Cereb Blood Flow Metab 21 : 202—210, 2001
10) Yokota C, Kuge Y, Inoue H, Tagaya M, Kito G, Susumu T, Tamaki N, Minematsu K : Post-ischemic cyclooxygenase-2 expression is regulated by the extent of cerebral blood flow reduction in non-human primates. Neurosci Lett 341 : 37—40, 2003
11) Minematsu K, Li L, Fisher M, Sotak CH, Davis MA, Fiandaca MS : Diffusion weighted magnetic resonance imaging : Rapid and quantitative detection of focal brain ischemia. Neurology 42 : 235—240, 1992
12) Yokota C, Kuge Y, Inoue H, Tamaki N, Minematsu K : Temporal and topographic profiles of cyclooxygenase-2 expression during 24 hours of focal brain ischemia in rats. Neurosci Lett 357 : 219—222, 2004
13) Lauritzen M, Jorgensen MB, Diemer NH, Gjedde

A, Hansen AJ : Persistent oligemia of rat cerebral cortex in the wake of spreading depression. Ann Neurol 12 : 469—474, 1982
14) Kuge Y, Hasegawa Y, Yokota C, Minematsu K, Hashimoto N, Miyake Y, Yamaguchi T : Effects of single and repetitive spreading depression on cerebral blood flow and glucose metabolism in cats : A pet study. J Neurol Sci 176 : 114—123, 2000
15) Woods RP, Iacoboni M, Mazziotta JC : Bilateral spreading cerebral hypoperfusion during spontaneous migraine headache. New Engl J Med 331 : 1689—1692, 1994

急性期局所脳虚血病態時の脳循環代謝に対するプロスタグランジン制御

横田　千晶[1,3]，久下　裕司[2]，長谷川泰弘[3]，井上　裕康[4]，多賀谷昌史[5]
鐙谷　武雄[6]，鬼頭　剛[7]，玉木　長良[8]，峰松　一夫[3]

[1]国立循環器病センター研究所脳血管障害研究室
[2]京都大学大学院薬学研究科病態機能分析学分野
[3]国立循環器病センター内科脳血管部門
[4]国立循環器病センター研究所薬理部
[5]国立大阪病院内科
[6]江別病院脳外科
[7](株) 新日本科学
[8]北海道大学大学院医学研究科核医学分野

我々は，急性期病態モデルとして，局所脳虚血モデルと spreading depression (SD) モデルを用いて，脳循環代謝変化と cyclooxygenase-2 (COX-2) 発現につき調べた．サル SD モデルにおいて，SD に伴う脳血流量の変化は一過性の脳血流上昇であり，持続的な血流低下を伴わなかった．SD 誘発サルの脳神経細胞には，COX-2 蛋白が発現していた．サル塞栓性脳梗塞モデルにおいて，虚血 24 時間までは主に脳神経細胞に COX-2 が発現し，特に脳糖代謝率が保たれている梗塞周囲領域での発現が増強していた．局所脳虚血ラット実験より，虚血周辺部と中心部では，COX-2 (mRNA，蛋白) 発現の時間経過と発現量，およびプロスタグランジン生成量は異なっていた．COX-2 蛋白は，神経細胞に発現していた．本研究により，急性期脳虚血病態と脳組織での COX-2 誘導およびプロスタグランジン産生は深く関連していることが明らかとなった．

キーワード：局所脳虚血，cyclooxygenase-2，サル，spreading depression

International Congress Series 1264 (2004) 191–196

ELSEVIER

www.ics-elsevier.com

Neuronal cyclooxygenase-2 induction associated with spreading depression and focal brain ischemia in primates

Chiaki Yokota[a,*], Yuji Kuge[b], Yasuhiro Hasegawa[c], Hiroyasu Inoue[d], Masafumi Tagaya[e], Takeo Abumiya[f], Go Kito[g], Nagara Tamaki[h], Kazuo Minematsu[c]

[a] *Cerebrovascular Laboratory, National Cardiovascular Center Research Institute, 5-7-1 Fujishirodai, Suita, Osaka 565-8565, Japan*

[b] *Department of Patho-functional Bioanalysis, Graduate School of Pharmaceutical Sciences, Kyoto University, Kyoto, Japan*

[c] *Cerebrovascular Division, National Cardiovascular Center Research Institute, 5-7-1 Fujishirodai, Suita, Osaka, Japan*

[d] *Department of Pharmacology, National Cardiovascular Center Research Institute, Suita, Osaka, Japan*

[e] *National Osaka Hospital, Osaka, Japan*

[f] *Hokkaido Ebetsu Hospital, Ebetsu, Japan*

[g] *Shin Nippon Biomedical Laboratories, Ltd., Kagashima, Japan*

[h] *Department of Nuclear Medicine, Graduate School of Medicine, Hokkaido University, Sapporo, Japan*

Abstract. We investigated pathophysiology of a primate model eliciting spreading depression (SD), as well as a primate thromboembolic model, by using PET. Immediately after the first SD, focal cortical hyperemia was demonstrated without being followed by spreading or persistent hypoperfusion. Cyclooxygenase-2 (COX-2) induction was detected in SD animals by microarray analysis. Immunoreactive neurons were observed in SD animals. In the thromboembolic model, cerebral blood flow (CBF) following 24 h of ischemia reduced to 20–40% in the ischemic temporal cortex as well as ischemic basal ganglia, while the reduction was 40–60% in the ischemic parietal cortex. Upregulation of COX-2 mRNA expression was observed after 2 h of ischemia, but disappeared by 24 h in the ischemic temporal cortex. In the ischemic parietal cortex, where CMRglc was preserved, COX-2 expression persisted even after 24 h of ischemia. In conclusion, we showed unique features of CBF changes associated with SD in primates. Neuronal COX-2 induction was demonstrated in SD animals as well as within potentially viable hypoperfused brain areas in primates.

Keywords: Primate; Spreading depression; Focal brain ischemia; Cyclooxygenase 2; PET

* Corresponding author. Tel.: +81-6-6833-5012; fax: +81-6-6872-8091.
E-mail address: cyokota@ri.ncvc.go.jp (C. Yokota).

0531-5131/
doi:10.1016/j.ics.2004.01.006

1. Introduction

Cortical spreading depression (SD) [1] has been suggested to play a significant role in the development of ischemic injury under conditions of focal brain ischemia in rat models [2,3]. As proposed by the Stroke Therapy Academic Industry Roundtable [4], nonhuman primate studies are required to clarify the pathophysiology of ischemic stroke and to verify the safety and efficacy of newly developed drugs that show promising results in rodents. In order to investigate the pathophysiology of acute ischemic stroke, we have developed a primate model eliciting SD, as well as a primate thromboembolic stroke model.

All procedures in this study were approved by our Institutional Animal Research Committee and were performed in accordance with the standards published by the National Research Council (Guide for the Care and Use of Laboratory Animals).

2. Material and methods

2.1. Spreading depression in a primate model

We used nine adult male cynomolgus monkeys. Animals were anesthetized with pentobarbital (0.1 mg/kg, i.p.). Anesthesia was maintained with an N_2O/O_2 (70%:30%) gas mixture inhalation under artificial ventilation through an experimental period. They were divided into two groups, such as normal control (group C, $n=3$) and SD-evoked animals (group SD, $n=6$).

SD was elicited by applying 3.3 mol/l potassium chloride (KCl) through a burr hole made in the left parietal skull [5]. Two other burr holes were made rostral to the hole for KCl application. DC potentials were monitored with microelectrodes inserted into the cortex to a depth of 1 mm through the burr holes, except the hole for KCl application.

Cerebral blood flow (CBF) was measured with PET and the ^{15}O-labeled water bolus injection method. A baseline CBF measurement was done once prior to application of KCl solution. CBF measurements were repeated five times, beginning 3 min after the first SD at intervals of approximately 15 min. After completion of the PET studies (at 120 min after KCl application), the brain tissues in group SD were quickly removed after exsanguination following perfusion with cold saline. Samples of brain tissues in group C were also obtained in the same manner as those in group SD. We investigated the gene expression profile associated with SD by a cDNA array system containing 9182 human elements, which was confirmed by RNA blot, immunoblot, and immunohistochemical analyses [6].

2.2. Thromboembolic stroke model in primates

Thromboembolic stroke was produced in male cynomolgus monkeys ($n=4$) as described previously [7]. CBF was measured with ^{15}O-labeled water before and 1, 2, 4, 6, and 24 h after embolization. CMRglc was measured with [^{18}F] FDG methods 24 h after embolization [8]. Lesion size and location was determined 24 h after embolization by the 2,3,5-triphenyl-tetrazolium chloride (TTC)-staining method.

For biochemical analyses of brain tissues in the thromboembolic stroke model, we used nine adult male cynomolgus monkeys; three monkeys served as normal control and the remaining six as ischemic animals [9]. Two hours after a single autologous blood clot

injection in three monkeys, or after the completion of the PET studies in the other monkeys with 24-h ischemia, brain tissues were perfused with cold saline, and the animals were sacrificed. Three normal controls were also sacrificed in the same manner. Expression ratios of cyclooxygenase-2 (COX-2) mRNA were calculated as ratios of COX-2 mRNA against those of normal brains. Cell injury was evaluated by incorporation of digoxigenin deoxy-uridine-5′ -triphosphate (dUTP) with the use of DNA polymerase I [10].

3. Results

3.1. SD in primates

SD waves were recorded in eight of the nine monkeys. Single episodes in three monkeys, twice in two, and six episodes in one were recorded in the rostral sites. In two of three animals with the caudal hole, one had eight episodes, and another had one in the caudal sites for chemical stimulation, while there were no SD waves in the rostral sites. The remaining one had two episodes in the rostral and six episodes in the caudal sites. Focal hyperemia was demonstrated adjacent to the site of the KCl application immediately after the first SD. Average cortical CBF in the ipsilateral hemisphere increased significantly immediately after the chemical stimulation ($p < 0.05$ by paired t-test), and the significant increase in CBF persisted throughout the experimental period of 2 h. In the contralateral hemisphere, no significant changes in CBF were observed.

As a result of microarray analysis, increases in normalized signals of gene expression above 1.5-fold was seen in the cyclooxygenase-2 (COX-2) gene (1.6-fold), and 265 genes were different by at least 1.3-fold between the two groups. COX-2 induction was

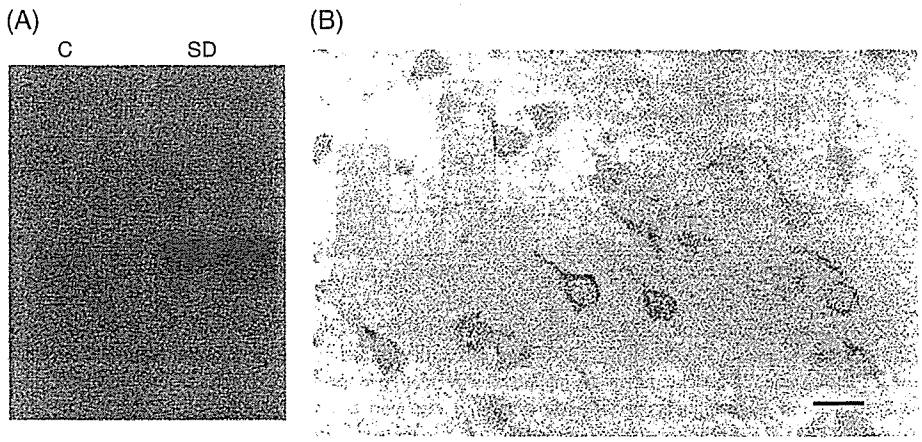

Fig. 1. Induction of COX-2 protein. (A) Immunoblot analysis shows a 70–72-kDa COX-2-immunoreactive band that is barely detectable in the group C (control), but clearly seen in the group SD. (B) Representative image of intense, immunoreactive neurons are shown in the animals with 6 SD episodes in the site rostral to the site of chemical stimulation. In these immunoreactive neurons, cell bodies and apical dendrites showed intense immunoreactivity. Scale bars: 100 μm.

confirmed by RNA blot, immunoblot (Fig. 1), and immunohistochemical analyses (Fig. 1). Intense immunoreactive neurons were induced in the animals with SDs.

3.2. Focal brain ischemia in primates

CBF in the temporal cortex and the basal ganglia decreased to <40% of the contralateral values 1 h after embolization, following further decline in CBF as well as CMRglc at 24 h of ischemia. These regions were consistently unstained with TTC, indicating that both temporal cortex and basal ganglia ipsilateral to the arterial embolization were regarded as the ischemic core. CBF was >40% of the contralateral values 1 h after embolization and recovered gradually with time in the parietal cortex ipsilateral to the embolization. No obvious TTC-unstained lesions were demonstrated in these regions, which implicated that the parietal cortex ipsilateral to the embolization was regarded as the ischemic penumbra. An increase in CMRglc at 24 h of ischemia compared with those in the contralateral regions, an uncoupling of CBF and CMRglc, was demonstrated in these regions.

The upregulation of COX-2 mRNA expression was observed at 2 h (expression ratio, 7.4), but disappeared by 24 h in the ischemic temporal cortex (Fig. 2), where cell injury was apparent by incorporation of dUTP. In the ischemic parietal cortex, where flow-metabolism uncoupling was observed, COX-2 mRNA was persistently induced even at

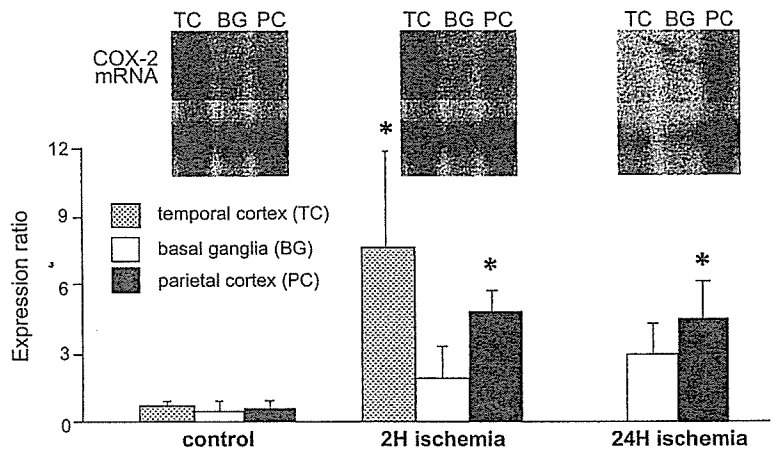

Fig. 2. RNA blot analysis of COX-2 expression. Autoradiograms of COX-2 (top) and glyceraldehyde-3-phosphate dehydrogenase (GAPDH) mRNA (bottom) from the following samples: normal control, 2-h ischemia on the ipsilateral side, 24-h ischemia on the ipsilateral side relative to the arterial embolization. Note that induced COX-2 expression is prominent in ischemic temporal and parietal cortices in 2-h ischemia. Upregulated expression of COX-2 mRNA was also shown in the ischemic parietal cortex in 24-h ischemia, while detection of COX-2 mRNA was faint in control. The diagram shows the expression ratio of COX-2 in each region. The expression ratio of the ischemic temporal cortex in 2-h ischemia was significantly higher than that in control ($*p<0.05$). Neither COX-2 nor GAPDH mRNA levels were determined in the ischemic temporal cortex in 24-h ischemia because of a reduction in both COX-2 and GAPDH mRNA levels. The expression ratio of the ischemic parietal cortex in 24-h ischemia was the same as that in 2-h ischemia, and both were significantly higher than in the normal control ($*p<0.05$).

24 h after ischemia (expression ratio, 4.7), and few damaged cells could be detected by incorporation of dUTP as well as in each region from the hemisphere contralateral to the clot injection. Intense COX-2 immunoreactivity was found in discrete neurons in the ischemic parietal cortex, although no significant increases in COX-2 protein level were shown either in the ischemic temporal or parietal cortices.

4. Discussion

The CBF pattern obtained in the SD model of primates differed from those obtained in other studies using rat and cat SD models [11,12]. The focal hyperemia was not followed by prolonged hypoperfusion. The changes in CBF during the SD phenomenon in primates also differed from those in patients with migraine [13,14]. These unique features of SD in this primate demand reappraisal of the hypothesis that SD contributes to the pathogenesis of human brain diseases. In biochemical analyses for brain tissues, COX-2 was induced in the cortices where SD was recorded, in accordance with previous observations in rodent models [15,16]. COX-2 was reported to play a role in mediating the increase in CBF produced by synaptic activity in the somatosensory cortex of mice [17].

We observed COX-2 expression during focal brain ischemia in a primate thromboembolic stroke model. In the ischemic core, in which a significant decrease in CBF was accompanied by reduced CMRglc, we observed upregulated COX-2 mRNA at 2-h ischemia with a decrease by 24 h. Disappearance of COX-2 at 24-h ischemia was parallel to a housekeeping GAPDH-mRNA reduction, indicating that ischemic injury was already apparent at 24-h ischemia in the temporal cortex and the basal ganglia. In the peri-infarct area, on the contrary, induced expression of COX-2 mRNA was still found at 24-h ischemia in the parietal cortex with a mild CBF reduction and maintained CMRglc. The results suggested that COX-2 expression might be regulated by the depth and duration of CBF reduction that is highly associated with local metabolic conditions.

The induction of neuronal COX-2 in brain tissues where SDs were elicited as well as in the ischemic cortices may participate in activity-dependent neural plasticity [18], because the metabolites of the arachidonic acid cascade are considered to play an important role in neuronal signaling [19,20]. Further studies describing the time course and topography of COX-2 expression, effects of a selective COX-2 antagonist given at various time-points after ischemia on ischemic brain damage, and prostanoids production downstream from COX-2 are required to clarify the role of COX-2 expression in ischemic brain injury.

Acknowledgements

This study was supported in part by a Grant-in-Aid for Scientific Research from the Japan Society for the Promotion of Science, by grants from the Takeda Medical Research Foundation, by the Mitsubishi Pharma Research Foundation, and by the Japan Heart Foundation.

References

[1] A.A.P. Leao, Spreading depression of activity in the cerebral cortex, J. Neurophysiol. 7 (1944) 359–390.
[2] K.A. Hossmann, Viability thresholds and the penumbra of focal ischemia, Ann. Neurol. 36 (1994) 557–565.

[3] K. Takano, L.L. Latour, J.E. Formato, R.A.D. Carano, K.G. Helmer, Y. Hasegawa, C.H. Sotak, M. Fisher, The role of spreading depression in focal ischemia evaluated by diffusion mapping, Ann. Neurol. 39 (1996) 308–318.
[4] Stroke Therapy Academic Industry Roundtable, Recommendations for standards regarding preclinical neuroprotective and restorative drug development, Stroke 30 (1999) 2752–2758.
[5] C. Yokota, Y. Kuge, Y. Hasegawa, M. Tagaya, T. Abumiya, N. Ejima, N. Tamaki, T. Yamaguchi, K. Minematsu, Unique profile of spreading depression in a primate model, J. Cereb. Blood Flow Metab. 22 (2002) 835–842.
[6] C. Yokota, H. Inoue, Y. Kuge, T. Abumiya, M. Tagaya, Y. Hasegawa, N. Ejima, N. Tamaki, K. Minematsu, Cyclooxygenase-2 expression associated with spreading depression in a primate model, J. Cereb. Blood Flow Metab. 23 (2003) 395–398.
[7] G. Kito, A. Nishimura, T. Susumu, R. Nagata, Y. Kuge, C. Yokota, K. Minematstu, Experimental thromboembolic stroke in cynomolgus monkey, J. Neurosci. Methods 105 (2001) 45–53.
[8] Y. Kuge, C. Yokota, M. Tagaya, Y. Hasegawa, A. Nishimura, G. Kito, N. Tamaki, N. Hashimoto, T. Yamaguchi, K. Minematsu, Serial changes in cerebral blood flow and flow-metabolism uncoupling in primates with acute thromboembolic stroke, J. Cereb. Blood Flow Metab. 21 (2001) 202–210.
[9] C. Yokota, Y. Kuge, H. Inoue, M. Tagaya, G. Kito, T. Susumu, N. Tamaki, K. Minematsu, Post-ischemic cyclooxygenase-2 expression is regulated by the extent of cerebral blood flow reduction in non-human primates, Neurosci. Lett. 341 (2003) 37–40.
[10] M. Tagaya, K.-F. Liu, B. Copeland, D. Seiffert, R. Engler, J.H. Garcia, G.J. del-Zoppo, DNA scission after focal brain ischemia: temporal differences in two species, Stroke 28 (1997) 1245–1254.
[11] M. Lauritzen, M.B. Jorgensen, N.H. Diemer, A. Gjedde, A.J. Hansen, Persistent oligemia of rat cerebral cortex in the wake of spreading depression, Ann. Neurol. 12 (1982) 469–474.
[12] Y. Kuge, Y. Hasegawa, C. Yokota, K. Minematsu, N. Hashimoto, Y. Miyake, T. Yamaguchi, Effects of single and repetitive spreading depression on cerebral blood flow and glucose metabolism in cats: a PET study, J. Neurol. Sci. 176 (2000) 114–123.
[13] J. Olesen, B. Larsen, M. Lauritzen, Focal hyperemia followed by spreading oligemia and impaired activation of rCBF in classic migraine, Ann. Neurol. 9 (1981) 344–352.
[14] R.P. Woods, M. Iacoboni, J.C. Mazziotta, Bilateral spreading cerebral hypoperfusion during spontaneous migraine headache, N. Engl. J. Med. 331 (1994) 1689–1692.
[15] S. Miettinen, F.R. Fusco, J. Yrjanheikki, R. Keinanen, T. Hirvonen, R. Roivainen, M. Narhi, T. Hokfelt, J. Koistinaho, Spreading depression and focal brain ischemia induce cyclooxygenase-2 in cortical neurons through *N*-methyl-D-aspartic acid-receptors and phospholipase A2, Proc. Natl. Acad. Sci. U. S. A. 94 (1997) 6500–6505.
[16] J. Koistinaho, S. Pasonen, J. Yrjanheikki, P.H. Chan, Spreading depression-induced gene expression is regulated by plasma glucose, Stroke 30 (1999) 114–119.
[17] K. Niwa, E. Araki, S.G. Morham, M.E. Ross, C. Iadecola, Cyclooxygenase-2 contributes to functional hyperemia in whisker-barrel cortex, J. Neurosci. 20 (2000) 763–770.
[18] K. Yamagata, K.I. Andreasson, W.E. Kaufmann, C.A. Barnes, P.F. Worley, Expression of a mitogen-inducible cyclooxygenase in brain neurons: regulation by synaptic activity and glucocorticoids, Neuron 11 (1993) 371–386.
[19] T. Shimizu, L.S. Wolfe, Arachidonic acid cascade and signal transduction, J. Neurochem. 55 (1990) 1–15.
[20] W.E. Kaufmann, P.F. Worley, J. Pegg, M. Bremer, P. Isakson, COX-2, a synaptically induced enzyme, is expressed by excitatory neurons at postsynaptic sites in rat cerebral cortex, Proc. Natl. Acad. Sci. U. S. A. 93 (1996) 2317–2321.

THE JOURNAL OF BIOLOGICAL CHEMISTRY
Vol. 279, No. 43, Issue of October 22, pp. 44756–44762, 2004
Printed in U.S.A.

Cell Type-specific Regulation of RhoA Activity during Cytokinesis*[S]

Received for publication, March 1, 2004, and in revised form, August 2, 2004
Published, JBC Papers in Press, August 12, 2004, DOI 10.1074/jbc.M402292200

Hisayoshi Yoshizaki‡§, Yusuke Ohba‡, Maria-Carla Parrini‡¶, Natalya G. Dulyaninova‖, Anne R. Bresnick‖, Naoki Mochizuki§, and Michiyuki Matsuda‡**

From the ‡Department of Tumor Virology, Research Institute for Microbial Diseases, Osaka University, Yamadaoka, Suita-shi, Osaka 565-0871, the §Department of Structural Analysis, National Cardiovascular Center Research Institute, Fujishirodai, Suita-shi, Osaka 565-8565, Japan, and the ‖Department of Biochemistry, Albert Einstein College of Medicine, Bronx, New York 10461

Rho family GTPases play pivotal roles in cytokinesis. By using probes based on the principle of fluorescence resonance energy transfer (FRET), we have shown that in HeLa cells RhoA activity increases with the progression of cytokinesis. Here we show that in Rat1A cells RhoA activity remained suppressed during most of the cytokinesis. Consistent with this observation, the expression of C3 toxin inhibited cytokinesis in HeLa cells but not in Rat1A cells. Furthermore, the expression of a dominant negative mutant of Ect2, a Rho GEF, or Y-27632, an inhibitor of the Rho-dependent kinase ROCK, inhibited cytokinesis in HeLa cells but not in Rat1A cells. In contrast to the activity of RhoA, the activity of Rac1 was suppressed during cytokinesis and started increasing at the plasma membrane of polar sides before the abscission of the daughter cells in both HeLa and Rat1A cells. This type of Rac1 suppression was shown to be essential for cytokinesis because a constitutively active mutant of Rac1 induced a multinucleated phenotype in both HeLa and Rat1A cells. Moreover, the involvement of MgcRacGAP/CYK-4 in this suppression of Rac1 during cytokinesis was shown by the use of a dominant negative mutant. Because ML-7, an inhibitor of myosin light chain kinase, delayed the cytokinesis of Rat1A cells and because Pak, a Rac1 effector, is known to suppress myosin light chain kinase, the suppression of the Rac1-Pak pathway by MgcRacGAP may play a pivotal role in the cytokinesis of Rat1A cells.

After chromosomal separation at the onset of anaphase, cytokinesis creates two daughter cells endowed with a complete set of chromosomes and cytoplasmic organelles. During this period, cortical actin and myosin II begin to move toward the equatorial region, where they form a contractile cleavage furrow (1–3). Rho family GTPases, which regulate a number of cell functions including gene expression and cell adhesion (4), also play a pivotal role in cytokinesis (2, 5, 6). Among them, RhoA has been shown to be necessary for cytokinesis in a variety of cell types including *Xenopus* and sand dollar eggs (7). Furthermore (8, 9), significant progress has been made in the identification of RhoA effectors during cytokinesis (5). One RhoA effector, Rho kinase/ROCK, stimulates myosin II regulatory light chain (MLC)[1] directly by phosphorylation and indirectly by the inhibition of myosin phosphatase (10, 11). Another RhoA effector, citron kinase, also phosphorylates and activates MLC (12). This phosphorylation of MLC is believed to lead to actomyosin contractility and thereby to cytokinesis. However, the role of RhoA in cytokinesis may not be identical in adherent cells and in eggs or poorly adherent cells; well adherent NRK and Swiss 3T3 cells undergo cell division in the presence of an inhibitor of Rho, C3 ribosyltransferase, suggesting that cytokinesis may proceed by a RhoA-independent mechanism in some cell types (13).

In addition to RhoA, Rac1, and Cdc42 have also been implicated in the cytokinesis of mammalian cells, based on the appearance of multinucleated cells among cells expressing constitutively active Rac1 or Cdc42 (14, 15). In agreement with this view, it has been speculated that low microtubule density at the equatorial region leads to the suppression of Rac1 (6). This suppression of Rac1 activity down-regulates Pak, a kinase known to phosphorylate and thereby suppress MLCK (16). Therefore, the suppression of Rac1 may also be involved in the contraction of the cleavage furrow.

The activity of Rho family GTPases is regulated by the balance between guanine nucleotide exchange factors (GEFs) and GTPase-activating proteins (GAPs); GEF activates Rho by catalyzing the uptake of GTP, whereas GAP stimulates the GTPase activity of Rho, leading to its inactivation. Molecular and genetic studies have shown that a mammalian Rho GEF, ECT2, and its *Drosophila melanogaster* ortholog, Pebble (PBL), are required for cytokinesis (17, 18). Recent studies have shown that these GEFs may be particularly important in the determination of the place and timing of cytokinesis (19, 20). In addition to the GEFs, GAPs also appear to play a critical role during cytokinesis. A GAP for the Rho family GTPases, MgcRacGAP/CYK-4, is a component of the central spindlin complex, which bundles microtubules in the central spindle (20–23). The inhibition of MgcRacGAP/CYK-4 by mutants or RNA interference inhibits cytokinesis, inducing multinucle-

* This work was supported in part by a grant for scientific research on priority areas (special) from the Ministry of Education, Science, Sports, and Culture of Japan and by a grant for comprehensive research on aging and health from the Ministry of Health, Labor, and Welfare. The costs of publication of this article were defrayed in part by the payment of page charges. This article must therefore be hereby marked "*advertisement*" in accordance with 18 U.S.C. Section 1734 solely to indicate this fact.

[S] The on-line version of this article (available at http://www.jbc.org) contains a figure.

¶ Fellow supported by the Japan Society for the Promotion of Science.

** To whom correspondence should be addressed: Dept. of Tumor Virology, Research Institute for Microbial Diseases, Osaka University, Yamadaoka, Suita-shi, Osaka 565-0871, Japan. Tel.: 81-6-6879-8316; Fax: 81-6-6879-8314; E-mail: matsudam@biken.osaka-u.ac.jp.

[1] The abbreviations used are: MLC, myosin II regulatory light chain; GEF, guanine nucleotide exchange factor; GAP, GTPase-activating protein; FRET, fluorescence resonance energy transfer; BrdUrd, bromo-2′-deoxyuridine; MLCK, myosin light chain kinase; NRK, normal rat kidney; CFP, green fluorescent protein; YFP, yellow fluorescent protein; CFP, cyan fluorescent protein; DMEM, Dulbecco's modified Eagle's medium; FBS, fetal bovine serum; PBS, phosphate-buffered saline; DIC, differential interference contrast.

ated cells (22, 23). MgcRacGAP/CYK-4 is 20–30-fold more active toward Rac1 and Cdc42 than toward RhoA (21), but becomes active toward RhoA upon phosphorylation by Aurora B (24). This MgcRacGAP/CYK-4-mediated RhoA suppression has been shown to be required for proper cortical activity during cytokinesis (25). Furthermore, PRC1, a human spindle-associated cyclin-dependent kinase substrate, binds to and inhibits the Cdc42 GAP activity of MgcRacGAP/CYK-4 (26). Therefore, at least three Rho family GTPases, RhoA, Rac1, and Cdc42, can function as potential targets of MgcRacGAP/CYK-4 during cytokinesis.

Because the precise spatio-temporal regulation of the Rho family GTPases is critical for the progression of cytokinesis, it is necessary to visualize changes in the activity of these GTPases in living cells. To this end, we developed probes for the Rho family GTPases based on the principle of fluorescent resonance energy transfer (FRET) (27, 28). By using these FRET-based probes, we have shown that the activities of RhoA, Rac1, and Cdc42 decrease upon entry into mitosis in HeLa cells (28). Although RhoA activity starts to increase after the initiation of cytokinesis, the activities of Rac1 and Cdc42 begin to increase at approximately the time of the abscission of daughter cells. Here we extended our previous study by using Rat1A cells in place of HeLa cells, and we demonstrated that RhoA activation at the onset of cytokinesis is not found in this cell type. In accord with this observation, the cytokinesis of Rat1A was not inhibited by inhibitors of RhoA. These observations indicate that the activation of and the requirement for RhoA during cytokinesis are cell type-specific.

EXPERIMENTAL PROCEDURES

FRET Probes, Plasmids, and Recombinant Adenoviruses—The FRET probes, designated as Raichu-Rac1 and Raichu-RhoA, have been described previously (27, 28). The cDNAs for Rac1-V12 and Rac1-N17 were expressed from a pIRM21-FLAG expression vector containing a FLAG tag and an internal ribosomal entry site followed by the cDNA of a red fluorescent protein, dsFP593, at the 5′- and 3′-side of the cloning site, respectively (27). An expression vector of a dominant negative form of Ect2, Ect2-N, was obtained from T. Miki (National Institutes of Health). A dominant negative mutant of MgcRacGAP was obtained from T. Kitamura (Institute for Medical Sciences, University of Tokyo) and was subcloned into pERedMit, which, at the 3′-side of the cloning site, contained an internal ribosomal entry site followed by the cDNA of Express Red (BD Biosciences) fused to mitochondria-targeting signal. cDNA of Pak T423E mutant was obtained from G. M. Bokoch (The Scripps Research Institute) (29) and subcloned into pERedNES, which contained an internal ribosomal entry site followed by the cDNA of Express Red fused to the nuclear export signal. Use of these two marker proteins with different targeting signals allows us to identify cells that express both of the expression plasmids. A recombinant adenovirus carrying C3 toxin cDNA, adeno-GFP-C3, and a control virus carrying GFP alone were obtained from H. Kurose (Kyusyu University, Fukuoka, Japan).

Cells—HeLa and NIH3T3 cells were purchased from the Human Science Research Resources Bank (Sennan-shi, Japan) and from the RIKEN Gene Bank (Wako-shi, Japan), respectively. Rat1A and NRK cells were gifts from Y. Nakabeppu (Kyushu University, Fukuoka, Japan) and H. Okayama (University of Tokyo, Tokyo, Japan), respectively. HeLa, NIH3T3, and Rat1A cells were maintained in DMEM (Sigma) supplemented with 10% FBS. NRK cells were maintained in DMEM supplemented with 5% FBS. Before cell imaging, DMEM was replaced with phenol red-free minimum Eagle's medium (Nissui, Tokyo, Japan) containing 10% FBS.

FRET Imaging of Rho Family GTPases in Living Cells—FRET imaging was performed essentially as described previously (28). Briefly, cells plated on a collagen-coated 35-mm diameter glass-base dishes (Asahi Techno Glass Co., Tokyo, Japan) were transfected with Raichu expression vectors and imaged every 2 min on an Olympus IX70 inverted microscope (Olympus Optical Co., Tokyo, Japan) that was equipped with a cooled CCD camera, CoolSNAP HQ (Roper Scientific, Trenton, NJ), and controlled by MetaMorph software (Universal Imaging, West Chester, PA) (30). For dual-emission ratio imaging of the Raichu probes, we used a 440AF21 excitation filter, a 455DRLP dichroic mirror, and two emission filters, 480AF30 for CFP and 535AF26 for YFP (Omega Optical Inc., Brattleboro, VT). Cells were illuminated with a 75-watt xenon lamp through a 12% ND filter (Olympus Optical) and a 100× oil immersion objective lens. The exposure time was 0.5 s when the binning of the CCD camera was set to 4 × 4. After background subtraction, the ratio image of YFP/CFP was created with MetaMorph software and was used to represent the efficiency of the FRET.

Roles of Rho Family GTPases in Cytokinesis—Cells were infected with recombinant adenoviruses carrying GFP or GFP-C3. Thirty six hours later, the cells were labeled with BrdUrd (Sigma) for 12 h. After fixation with 70% ethanol, the cells were permeabilized with 0.1% Tween 20, followed by incubation in PBS containing 30 μg/ml DNase I (Roche Diagnostics) for 1 h. BrdUrd incorporated into the nucleus was detected with anti-BrdUrd antibody (BD Biosciences), followed by Alexa 546-conjugated anti-mouse IgG antibody (Molecular Probes, Inc., Eugene, OR). More than 100 cells that were positive for both BrdUrd and GFP were analyzed to identify the multinucleated phenotype. In other experiments, the cells were transfected with pIRM21-derived expression plasmids of Rho family GTPases or pERed-derived expression plasmids, and 48 h later, the cells expressing marker proteins were analyzed to identify the multinucleated phenotype.

Microinjection of C3 Toxin—The cDNA of C3 toxin was inserted into pGEX-6P (Amersham Biosciences). The purification of C3 was performed according to the manufacturer's protocol. Briefly, glutathione *S*-transferase-fused C3 was purified on a glutathione-Sepharose column from the cell lysates of *Escherichia coli* expressing pGEX-6P-C3. C3 was excised from glutathione *S*-transferase with PreScission protease, followed by dialysis against PBS. Cells in the metaphase were microinjected with 0.1 mg/ml C3 in PBS or with PBS alone and were analyzed to identify the multinucleated phenotype as described previously (13).

Effect of Kinase Inhibitors on Cytokinesis—Cells were treated with 40 μM Y-27632 (Calbiochem) for 4 h, 40 μM ML-7 (Calbiochem) for 5 min, or 100 μM blebbistatin (Toronto Research Chemicals Inc., North York, Ontario, Canada) for 1 min. Then, in the continuing presence of the inhibitors, cells in metaphase were identified, and such cells were recorded by DIC images created every 30 s in the case of the Rat1a cells and every 1 min in the case of the HeLa cells. By using these DIC images, the diameter of the contractile ring was measured and plotted to obtain the time course. Each time course was fitted to an exponential curve with GraFit software (Erithacus Software Ltd., Horley, UK), by which the maximum velocity and the half-time ($\tau_{1/2}$) of cleavage furrow contraction were calculated.

RESULTS AND DISCUSSION

Changes in the Activity of RhoA and Rac1 in Rat1A Cells Progressing from the G_2 to the G_1 Phase—To examine whether the changes in the activity of RhoA and Rac1 described in HeLa cells could be generalized to other cell types, we monitored spatio-temporal changes in the activities of RhoA and Rac1 by using Rat1A cells progressing from the G_2 to the G_1 phase, as described previously (28). Briefly, Rat1A cells expressing Raichu-RhoA or Raichu-Rac1 were excited at 440 nm and imaged for CFP and YFP at 475 and 530 nm, respectively. The intensity ratio YFP/CFP was used to represent the FRET efficiency of the probes, which reflects the GTP/GDP ratio on each probe. Because Raichu probes are regulated in a manner similar to that of authentic GTPases, the FRET value at each pixel of the digital image reflects the activity of the corresponding GTPase (28). Images of differential interference contrast and YFP-tagged actin were also obtained to follow the morphological changes.

At prophase, the activities of RhoA and Rac1 started decreasing, reaching a nadir at telophase, and gradually increased upon exit from the M phase (Fig. 1*A*). The activities were then averaged for the entire region of each Rat1A cell and compared with those of HeLa cells (Fig. 1*B*). RhoA activity started increasing at late telophase in Rat1A cells, whereas it did so in anaphase in the HeLa cells. The time course of the change in the activity of Rac1 was very similar between Rat1A cells and HeLa cells. In order to follow changes in activity over a long period of ~16 h, the objective lens was focused on the basal plasma membrane before imaging and was fixed during the

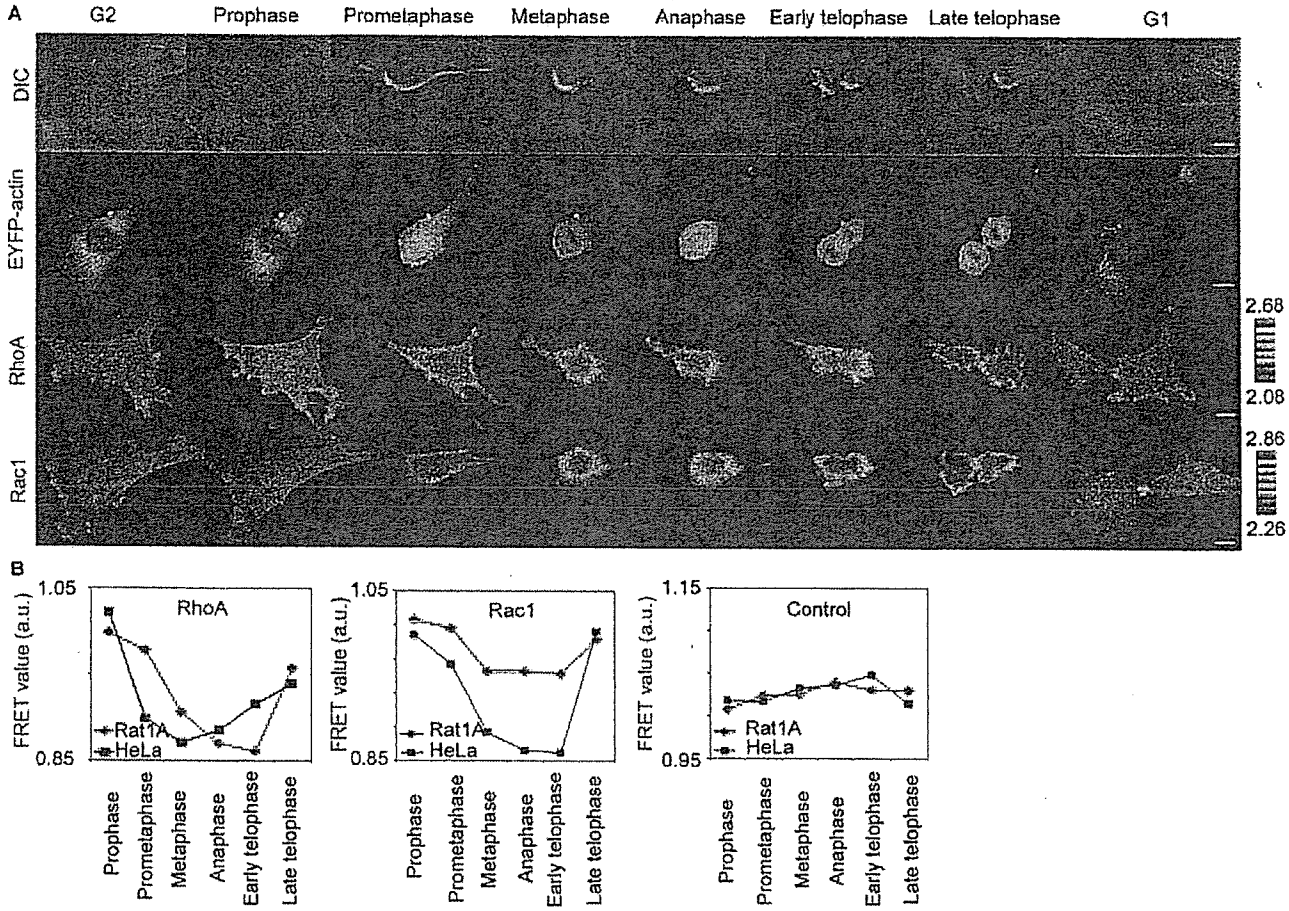

FIG. 1. **The activity of Rho family GTPases in HeLa cells progressing from the G_2 to the G_1 phase.** *A*, Rat1A cells were infected with recombinant adenoviruses for the expression of Raichu-RhoA and Raichu-Rac1, as indicated at *left*. CFP, YFP, and DIC images were obtained every 1 min with a time-lapse epifluorescent microscope. A ratio image of YFP/CFP was used to represent the FRET efficiency. The stages of the cell cycle were determined by the DIC images. Representative FRET images are shown at each stage of the cell cycle denoted at the *top* of the figure. The upper and lower limits of the ratio range are shown at the *right* of each panel. At least four similar images were obtained for each probe, and a representative image is used here. *B*, in the Rat1A cells from the images in *A*, the net intensities of YFP and CFP in each cell were measured in order to calculate the averaged YFP/CFP emission ratio. The HeLa cell experiments were performed in essentially the same manner as the Rat1A cell experiments. Because the basal level of the emission ratio varies from cell to cell, the relative emission ratio to that of the G_2 phase is used as an arbitrary unit (*a.u.*). As a control, we used Raichu-Pak-Rho as described (28).

entire experiment. Thus, upon the rounding of the cells during mitosis, the images always became out of focus. To obtain clearer images, we looked for cells that had entered into mitosis, and we acquired their images by continuously focusing the lens at the middle depth of the cells (Fig. 2*A*). The progression of cytokinesis was followed by measuring the breadth of the cells at the cleavage furrow. The averaged RhoA activity increased, whereas the constriction proceeded in HeLa cells, and in Rat1A cells, RhoA activity reached a nadir in the late phase of cytokinesis, slightly before the appearance of the mitotic midbody. We performed similar experiments with NRK and NIH3T3 cells and found that NRK cells behaved in a manner similar to that of HeLa cells, whereas NIH3T3 cells behaved in a manner similar to that of Rat1A cells (Fig. 2*B*). These observations suggest that the role of RhoA in cytokinesis is cell type-specific.

The changes in the activity of Rac1 were indistinguishable among HeLa, Rat1A, NRK, and NIH3T3 cells (Fig. 3). Suppression of Rac1 activity was most prominent at the cleavage furrow, and the increase in activity was initiated at the polar ends of the plasma membrane in both cell types.

Inhibition of Cytokinesis of HeLa and NRK Cells but Not of Rat1A and NIH3T3 Cells by C3—The lack of increase in RhoA activity during cytokinesis suggested its dispensability in the cytokinesis of Rat1A cells and NIH3T3 cells. To address this issue, we examined the effect of C3 toxin on cytokinesis. The effectiveness of C3 toxin delivered by a recombinant adenovirus was first confirmed by the loss of actin stress fibers in both HeLa and Rat1A cells.[2] To exclude cells that were G_1-arrested by the inactivation of Rho family GTPases (31), we stained the cells with BrdUrd, and we determined the number of multinucleated cells among those positive for both BrdUrd and GFP (Fig. 4*A*). The expression of GFP-C3 significantly induced the multinucleated phenotype in more than 50% of the HeLa cells but only in 10% of the Rat1A cells and 18% of the NIH3T3 cells. We could not perform a similar experiment by using NRK cells because of the toxicity of the recombinant adenovirus carrying GFP-C3 to this cell type. Therefore, we examined the effect of C3 by microinjecting purified C3 toxin into the cytoplasm at metaphase (Fig. 4*B*). Cytokinesis was remarkably inhibited in HeLa and NRK cells and was slightly disturbed in Rat1A cells by this manipulation. These results suggest that the requirement of RhoA for cytokinesis was less flexible in

[2] H. Yoshizaki and M. Matsuda, unpublished results.

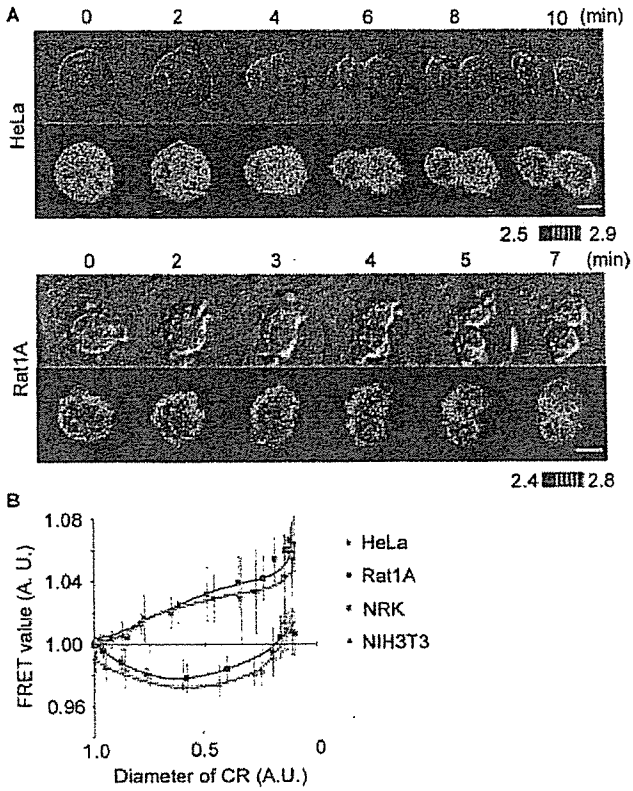

FIG. 2. **Changes in the activity of RhoA during cytokinesis.** *A*, HeLa cells or Rat1A cells expressing Raichu-RhoA were photographed as in Fig. 1*A*, except that the fluorescent images were focused on the contour of the cells and subjected to median filtering in order to reduce noise. The elapsed time and the phases are denoted at the *top* of the figure. Time zero is set to metaphase. *B*, the net intensities of YFP and CFP in each cell were measured in order to calculate the average emission ratio. The progression of cytokinesis was monitored by a decrease in the diameter of the contractile ring (*CR*). The *abscissa* shows the diameter of contractile ring in arbitrary units (*A.U.*), the value of which varies from 1 at the initiation to 0 at the end of cytokinesis. NRK cells and NIH3T3 cells expressing Raichu-RhoA were imaged, and the emission ratio (YFP/CFP) was obtained as in *A*. *Bars* indicate *error bars* from five cells.

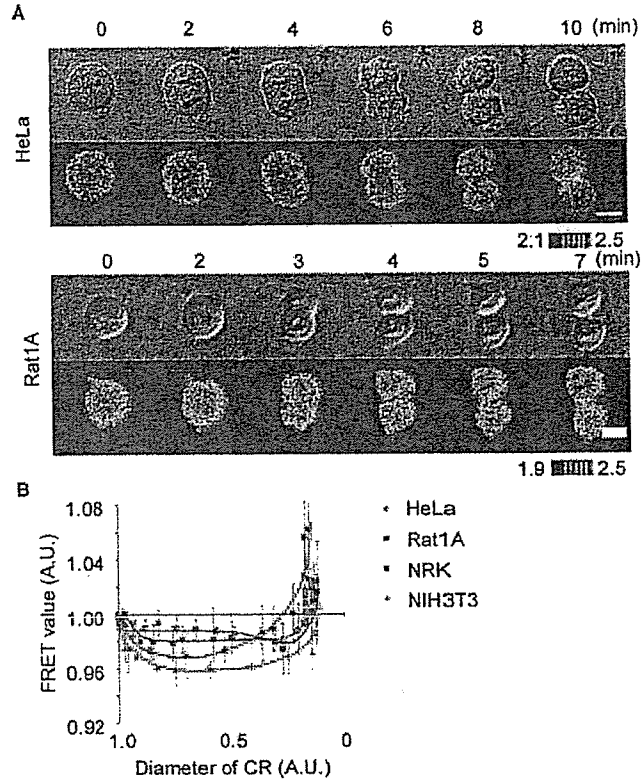

FIG. 3. **Changes in the activity of Rac1 during cytokinesis.** *A*, HeLa cells or Rat1A cells expressing Raichu-Rac1 were photographed as in Fig. 1*A*, except that the fluorescent images were focused on the contour of the cells and subjected to median filtering in order to reduce noise. The elapsed time and the phases are denoted at the *top* of the figure. The time 0 is set to metaphase. *B*, the net intensities of YFP and CFP in each cell were measured in order to calculate the averaged emission ratio. The progression of cytokinesis was analyzed as described in Fig. 2*B*. *A.U.*, arbitrary units.

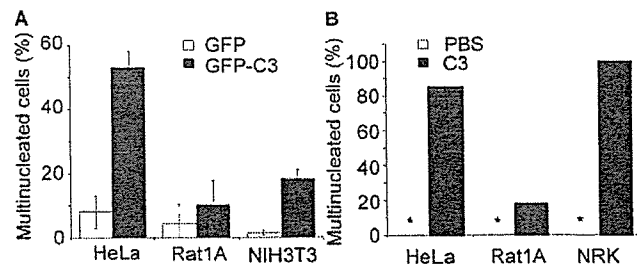

FIG. 4. **Cell type-dependent requirement of RhoA for cytokinesis.** *A*, HeLa cells, NIH3T3 cells, and Rat1A cells were infected with recombinant adenoviruses encoding GFP-C3 or GFP. Twenty four hours after infection, the cells were labeled with bromodeoxyuridine. Forty eight hours after adenovirus infection, more than 100 cells that were positive for both bromodeoxyuridine and GFP were analyzed to identify the multinucleated phenotype. Independent experiments were performed four times for HeLa and Rat1A cells and twice for NIH3T3 cells. Averaged data are shown with S.D. *B*, cells at metaphase were microinjected with C3 or PBS and were examined for the multinucleated phenotype. Fifteen cells were counted in every microinjected group. *Asterisks* indicate that no multinucleated cells were observed under that condition.

HeLa and NRK cells than in Rat1A cells and NIH3T3 cells. O'Connell *et al.* (13) have shown that the microinjection of C3 inhibits cytokinesis in HeLa cells but not in NRK cells and Swiss 3T3 cells. The discrepancy regarding the effects on NRK cells may have been due to the difference in the origin of NRK cells, the culturing conditions, or the concentration of C3. In any case, the effect of C3 on cytokinesis appeared to be dependent on the cellular context.

Role of the Suppression of Rac1 Activity in Cytokinesis—Next, we addressed the role of the suppression of Rac1 during cytokinesis. To this end, we expressed constitutively active or dominant negative mutants of Rac1 (Fig. 5*A*). The expression of Rac1-G12V significantly increased the number of multinucleated cells in both HeLa and Rat1A cells. This observation agreed with the results of previous reports, *i.e.* it was found that constitutively active Rac1 induced multinucleated cells in HeLa and porcine aortic endothelial cells (14, 15). In contrast to the constitutively active mutant, Rac1-T17N did not increase the number of multinucleated cells to a detectable level. This observation again agreed with those of previous reports (2, 21) showing that a loss of the function of Rac1 did not inhibit cytokinesis.

Among many effector molecules of Rac1, Pak may be involved in the regulation of cytokinesis. Microinjection of Pak inhibits cleavage furrow ingression of *Xenopus* egg (32). Pak phosphorylates and thereby inhibits MLCK (16, 33), which is known to promote cytokinesis through phosphorylation of myosin II (34). We found that expression of a constitutively active Pak1 mutant, Pak-T423E, significantly increased the number of multinucleated cells both in HeLa and NIH3T3 cells (Fig.

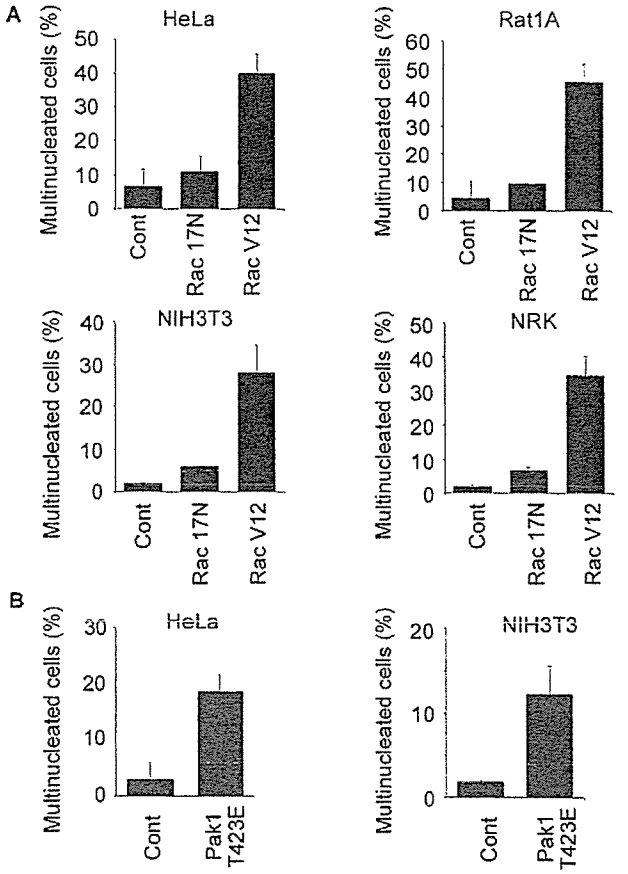

FIG. 5. **Role of Rac1 and Pak1 on cytokinesis.** *A*, HeLa cells, Rat1A cells, NRK cells, and NIH3T3 cells were transfected with constitutively active or the dominant negative mutant of GFP-Rac1 and were analyzed to identify the multinucleated phenotype as in Fig. 4. *B*, cells were transfected with a plasmid encoding constitutively active Pak1, Pak1 T423E, and analyzed for the multinucleated phenotype. *Cont*, control.

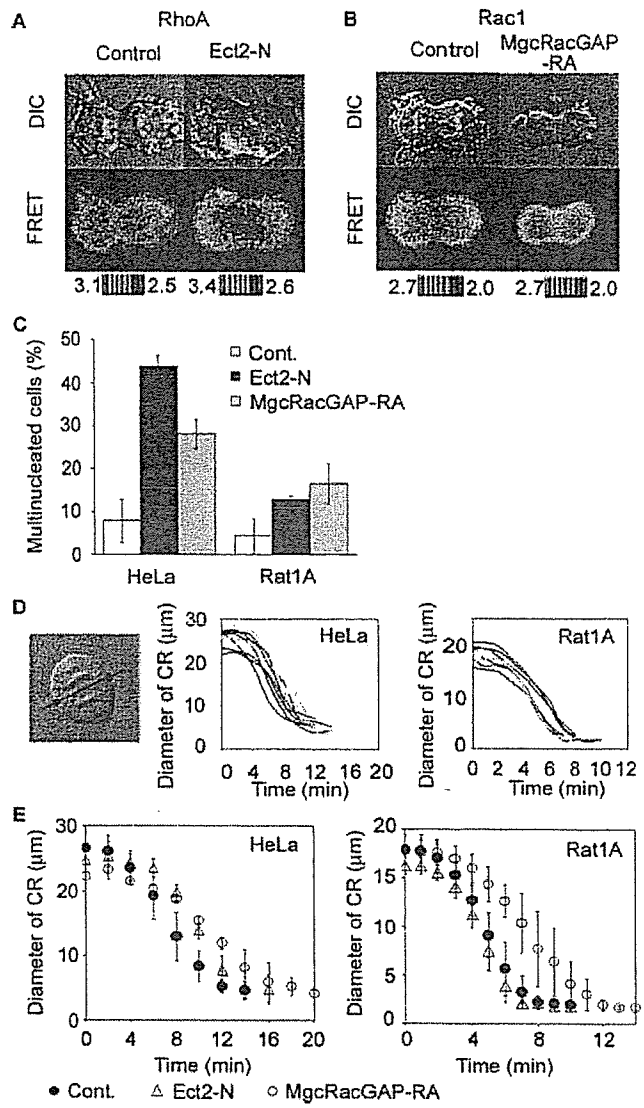

FIG. 6. **Effect of dominant negative mutants of Ect2 and MgcRacGAP/CYK-4.** *A*, HeLa cells expressing Ect2-N and Raichu-RhoA were imaged as in Fig. 2*A*. *B*, HeLa cells expressing MgcRacGAP-RA and Raichu-Rac1 were imaged as in Fig. 3*A*. *C*, HeLa cells and Rat1A cells were transfected with Ect2-N and MgcRacGAP-RA and were analyzed to identify the multinucleated phenotype as in Fig. 4. *D*, time-lapse analysis of cytokinesis in HeLa and Rat1A cells. The diameter of the contractile ring was measured as illustrated in the *left panel*. The *right panel* shows the aligned time courses of cleavage furrow constriction in control cells (n = 10). *E*, HeLa and Rat1A cells were mock-transfected or transfected with pEGFP-C1-Ect2-N4 or pEredMit-MgcRacGAP-RA and were observed for cytokinesis. *Cont.*, control. The averaged time courses are shown ($n > 4$).

5*B*). Thus, a decrease in Rac1 activity and the resulting suppression of Pak1 appear to be essential steps of cytokinesis in a variety of cell types.

Inhibition of Cytokinesis by Dominant Negative Mutants of Ect2 and MgcRacGAP/CYK-4—We further studied the mechanism of changes in the activity of Rho family GTPases during cytokinesis. For this purpose, we utilized dominant negative mutants of Ect2 and MgcRacGAP/CYK-4, which have been shown to regulate cytokinesis (18, 22, 23, 25). In cells expressing the dominant negative mutant of Ect2, Ect2-N, the increase in RhoA activity was suppressed at the cleavage furrow but not at the plasma membrane of polar sides (Fig. 6*A*). This observation agrees with the previously demonstrated recruitment of Ect2 to the cleavage furrow during cytokinesis (18) and suggests that multiple Rho GEFs are activated during cytokinesis. In cells expressing the dominant negative mutant of MgcRacGAP, MgcRacGAP-RA, Rac1 activity was not decreased at the cleavage furrow of HeLa cells, indicating that the suppression of Rac1 activity during cytokinesis was primarily mediated by the recruitment of MgcRacGAP (Fig. 6*B*).

To determine the effect of these mutants on cytokinesis quantitatively, we scored the number of multinucleated cells in the presence or absence of GFP-Ect2-N or MgcRacGAP-RA (Fig. 6*C*). Both GFP-Ect2-N and MgcRacGAP-RA increased the number of the multinucleated cells in HeLa cells. The effect of these mutants on Rat1A cells was marginal in this assay. Therefore, to examine the effect of these mutants on cytokinesis more directly, we measured the diameter of the contractile ring as shown by DIC images created during cytokinesis, and we calculated the maximum velocity of its shortening and the half-time of cytokinesis. The half-life of the shortening of the contractile ring was 7.2 min in the HeLa cells and 4.7 min in the Rat1A cells (Fig. 6*D*). In the presence of GFP-Ect2-N and MgcRacGAP-RA, the half-life of the shortening of the contractile ring was increased to 9.6 and 11.2 min, respectively, in HeLa cells (Fig. 6*E*). In Rat1A cells, however, only MgcRacGAP-RA increased the half-life of the contractile ring shortening to 7.1 min. These observations suggest the following conclusions. First, the increase in RhoA activity at the cleavage

furrow of HeLa cells was primarily mediated by Ect2. Second, the decrease in Rac1 activity at the cleavage furrow was primarily mediated by MgcRacGAP. Third, the activation of RhoA was not essential for the cytokinesis of Rat1A cells. Fourth, in Rat1A cells, suppression of Rac1 plays a more critical role in cytokinesis than activation of RhoA.

Recently, it has been shown that increases in RhoA activity are responsible for cortical rigidity (35). Diffuse increases in RhoA activity at the plasma membrane may play a role in this increased cortical rigidity. However, the results obtained with GFP-Ect2-N seem to indicate that such an increase at the cortex is not sufficient for cytokinesis, unless it is accompanied by an increase in RhoA activity at the cleavage furrow. More importantly, these results demonstrated that the inhibition of cytokinesis by C3 or GFP-Ect2-N in each cell type was closely correlated with an increase in RhoA activity during cytokinesis, as observed by the Raichu probes used here.

Notably, our observations are not necessarily in conflict with the recent finding that MgcRacGAP/CYK-4 phosphorylated by Aurora B acts on RhoA at the time of the abscission of daughter cells (24, 25). Because of the limitation in the resolution of the FRET images, we were unable to conclude whether or not RhoA was suppressed at the spindle midbody at the time of abscission.

Role of ROCK and MLCK on the Cytokinesis of HeLa and Rat1A Cells—To understand further the role of Rho family GTPases in the cytokinesis of HeLa and Rat1A cells, we tested the effects of various inhibitors that have been shown to disturb cytokinesis. First, we tested the effects of blebbistatin, an inhibitor of myosin II (36), because cytokinesis can proceed in a myosin II-independent manner in *Dictyostelium discoideum* (37). As shown in Fig. 7, blebbistatin abrogated the cytokinesis of both HeLa and Rat1A cells. Thus, we proceeded to examine the contribution of ROCK and MLCK, which can induce actomyosin contraction by the phosphorylation of the light chain of myosin II (2). To this end, we treated the cells with Y27632, an inhibitor of ROCK, or ML-7, an inhibitor of MLCK. In HeLa cells, the effect of ML-7 was insignificant, whereas Y-27632 markedly delayed the velocity of cleavage furrow ingression, as reported previously (38). In contrast, ML-7, but not Y27632 significantly inhibited the cleavage furrow ingression of Rat1A cells. Therefore, a relief of Pak suppression seemed to lead to MLCK-promoted cytokinesis in Rat1A cells, as suggested previously (6). One of our co-authors (39) has recently reported an essential role of MLCK in the normal spindle morphology and chromosomal alignment of mitotic HeLa cells by using dominant negative mutants of MLCK. In these HeLa cells expressing the dominant negative MLCK mutants, the frequency of the multinucleated cells was up to 11%, whereas the percentage of multinucleated cells exceeded 50% in the presence of C3 (Fig. 4). In addition, the effect of the dominant negative mutants of MLCK on the velocity of cleavage furrow ingression was markedly weaker than that of Y-27632 (supplemental figure). Therefore, we concluded that the effect on MLCK was prominent in metaphase but less remarkable during cytokinesis in HeLa cells. Altogether, cytokinesis of HeLa cells seems to be more resistant to the inhibition of MLCK than Rat1A cells.

In conclusion, this study revealed that there are at least two pathways leading to actomyosin contraction and the resulting constriction of the cleavage furrow. The contribution of each pathway may depend on the cellular context. For example, the Ect2-RhoA-ROCK pathway is predominant in HeLa cells, whereas the MgcRacGAP/CYK-4-Rac1-Pak-MLCK pathway plays a more important role in the cytokinesis of Rat1A cells. Such differences in the mechanism of cytokinesis may in turn have generated the observed discrepancy in the requirement of RhoA for cytokinesis.

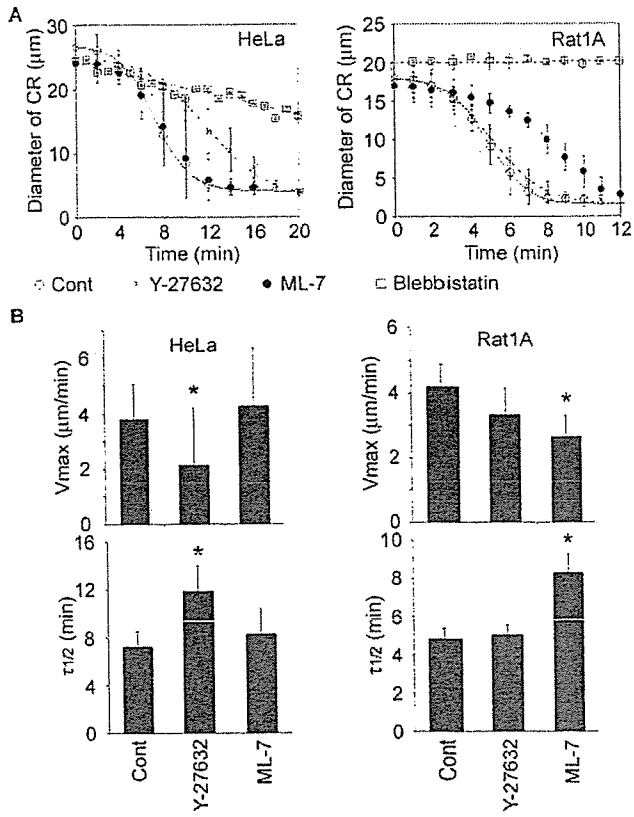

FIG. 7. **Differential role of ROCK and MLCK on the cytokinesis of HeLa and Rat1A cells.** *A*, HeLa and Rat1A cells untreated or treated with Y-27632, ML-7, or blebbistatin were observed for cytokinesis, as described in Fig. 6. The averaged time courses are shown ($n > 6$). *Cont.*, control. *B*, each time course was fitted to an exponential curve with GraFit software, by which the maximum velocity and the half-time ($\tau_{1/2}$) of cleavage furrow contraction were calculated; the results are shown as the mean ± S.D. *, $p < 0.005$ relative to the control.

Acknowledgments—We thank T. Miki, T. Kitamaura, H. Kurose, J. Miyazaki, Y. Nakabeppu, G. M. Bokoch, and H. Okayama for their provision of reagents, members of the Matsuda laboratory for helpful discussions, and N. Yoshida, N. Fujimoto, and Y. Matsuura for their technical assistance.

Note Added in Proof—Following acceptance of this manuscript, a complementary study was published that provides further genetic support for our proposal that MgcRacGAP/CYK-4/RacGAP50C suppresses Rac during cytokinesis (D'Avino, P. P., Savoian, M. S., and Glover, D. M. (2004) *J. Cell Biol.* **166**, 61–71).

REFERENCES

1. Mabuchi, I. (1986) *Int. Rev. Cytol.* **101**, 175–213
2. Glotzer, M. (2001) *Annu. Rev. Cell Dev. Biol.* **17**, 351–386
3. Glotzer, M. (2004) *J. Cell Biol.* **164**, 347–351
4. Bishop, A. L., and Hall, A. (2000) *Biochem. J.* **348**, 241–255
5. Prokopenko, S. N., Saint, R., and Bellen, H. J. (2000) *J. Cell Biol.* **148**, 843–848
6. Mandato, C. A., Benink, H. A., and Bement, W. M. (2000) *Cell Motil. Cytoskeleton* **45**, 87–92
7. Drechsel, D. N., Hyman, A. A., Hall, A., and Glotzer, M. (1997) *Curr. Biol.* **7**, 12–23
8. Kishi, K., Sasaki, T., Kuroda, S., Itoh, T., and Takai, Y. (1993) *J. Cell Biol.* **120**, 1187–1195
9. Mabuchi, I., Hamaguchi, Y., Fujimoto, H., Morii, N., Mishima, M., and Narumiya, S. (1993) *Zygote* **1**, 325–331
10. Amano, M., Ito, M., Kimura, K., Fukata, Y., Chihara, K., Nakano, T., Matsuura, Y., and Kaibuchi, K. (1996) *J. Biol. Chem.* **271**, 20246–20249
11. Kosako, H., Yoshida, T., Matsumura, F., Ishizaki, T., Narumiya, S., and Inagaki, M. (2000) *Oncogene* **19**, 6059–6064
12. Yamashiro, S., Totsukawa, G., Yamakita, Y., Sasaki, Y., Madaule, P., Ishizaki, T., Narumiya, S., and Matsumura, F. (2003) *Mol. Biol. Cell* **14**, 1745–1756
13. O'Connell, C. B., Wheatley, S. P., Ahmed, S., and Wang, Y. L. (1999) *J. Cell Biol.* **144**, 305–313
14. Dutartre, H., Davoust, J., Gorvel, J. P., and Chavrier, P. (1996) *J. Cell Sci.* **109**, 367–377
15. Muris, D., Verschoor, T., Divecha, N., and Michalides, R. (2002) *Eur. J. Cancer*

38, 1775–1782
16. Sanders, L. C., Matsumura, F., Bokoch, G. M., and de Lanerolle, P. (1999) *Science* **283**, 2083–2085
17. Prokopenko, S. N., Brumby, A., O'Keefe, L., Prior, L., He, Y., Saint, R., and Bellen, H. J. (1999) *Genes Dev.* **13**, 2301–2314
18. Tatsumoto, T., Xie, X., Blumenthal, R., Okamoto, I., and Miki, T. (1999) *J. Cell Biol.* **147**, 921–928
19. Mishima, M., and Glotzer, M. (2003) *Curr. Biol.* **13**, R589–R591
20. Somers, W. G., and Saint, R. (2003) *Dev. Cell* **4**, 29–39
21. Jantsch-Plunger, V., Gonczy, P., Romano, A., Schnabel, H., Hamill, D., Schnabel, R., Hyman, A. A., and Glotzer, M. (2000) *J. Cell Biol.* **149**, 1391–1404
22. Hirose, K., Kawashima, T., Iwamoto, I., Nosaka, T., and Kitamura, T. (2001) *J. Biol. Chem.* **276**, 5821–5828
23. Mishima, M., Kaitna, S., and Glotzer, M. (2002) *Dev. Cell* **2**, 41–54
24. Minoshima, Y., Kawashima, T., Hirose, K., Tonozuka, Y., Kawajiri, A., Bao, Y. C., Deng, X., Tatsuka, M., Narumiya, S., May, W. S., Nosaka, T., Semba, K., Inoue, T., Satoh, T., Inagaki, M., and Kitamura, T. (2003) *Dev. Cell* **4**, 549–560
25. Lee, J. S., Kamijo, K., Ohara, N., Kitamura, T., and Miki, T. (2004) *Exp. Cell Res.* **293**, 275–282
26. Ban, R., Irino, Y., Fukami, K., and Tanaka, H. (2004) *J. Biol. Chem.* **279**, 16394–16402
27. Itoh, R. E., Kurokawa, K., Ohba, Y., Yoshizaki, H., Mochizuki, N., and Matsuda, M. (2002) *Mol. Cell. Biol.* **22**, 6582–6591
28. Yoshizaki, H., Ohba, Y., Kurokawa, K., Itoh, R. E., Nakamura, T., Mochizuki, N., Nagashima, K., and Matsuda, M. (2003) *J. Cell Biol.* **162**, 223–232
29. Sells, M. A., Knaus, U. G., Bagrodia, S., Ambrose, D. M., Bokoch, G. M., and Chernoff, J. (1997) *Curr. Biol.* **7**, 202–210
30. Miyawaki, A., Llopis, J., Heim, R., McCaffery, J. M., Adams, J. A., Ikura, M., and Tsien, R. Y. (1997) *Nature* **388**, 882–887
31. Welsh, C. F., Roovers, K., Villanueva, J., Liu, Y., Schwartz, M. A., and Assoian, R. K. (2001) *Nat. Cell Biol.* **3**, 950–957
32. Rooney, R. D., Tuazon, P. T., Meek, W. E., Carroll, E. J., Hagen, J. J., Gump, E. L., Monnig, C. A., Lugo, T., and Traugh, J. A. (1996) *J. Biol. Chem.* **271**, 21498–21504
33. Bokoch, G. M. (2003) *Annu. Rev. Biochem.* **72**, 743–781
34. Poperechnaya, A., Varlamova, O., Lin, P. J., Stull, J. T., and Bresnick, A. R. (2000) *J. Cell Biol.* **151**, 697–708
35. Maddox, A. S., and Burridge, K. (2003) *J. Cell Biol.* **160**, 255–265
36. Straight, A. F., Cheung, A., Limouze, J., Chen, I., Westwood, N. J., Sellers, J. R., and Mitchison, T. J. (2003) *Science* **299**, 1743–1747
37. Gerisch, G., and Weber, I. (2000) *Curr. Opin. Cell Biol.* **12**, 126–132
38. Kosako, H., Goto, H., Yanagida, M., Matsuzawa, K., Fujita, M., Tomono, Y., Okigaki, T., Odai, H., Kaibuchi, K., and Inagaki, M. (1999) *Oncogene* **18**, 2783–2788
39. Dulyaninova, N. G., Patskovsky, Y. V., and Bresnick, A. R. (2004) *J. Cell Sci.* **117**, 1481–1493

トピックス

赤ワインに含まれるポリフェノール・レスベラトロールに関する最近の話題

レスベラトロールは赤ワインに含まれる抗酸化作用を持つフィトアレキシン(抗菌性物質)である．レスベラトロールは中等度のワイン消費が心血管病，脳卒中，痴呆の危険度と負の相関を示す，いわゆる「フレンチパラドックス」に関与する物質と考えられてきた．我々は最近，レスベラトロールが核内受容体PPAR(peroxisome proliferators activated receptor)αとPPARγを選択的に活性化すること，さらにPPARα活性化が脳保護効果をもたらすことを見いだした[1]．これらの知見は「フレンチパラドックス」を説明する新しい作用機構を提供すると考えている．一方で，レスベラトロールは寿命延長効果を持つカロリー制限模倣物質であること[2]，オレイルエタノールアミドがPPARαの新しい内因性リガンドであり，その活性化によって食欲をコントロールすること[3]が報告されている．そこでこれらの知見を含めて，今後の展望とともに紹介したい．

PPARはビタミンD受容体やグルココルチコイド受容体と同様，核内受容体ファミリーに属し，現在3種類のサブタイプα，γ，δ(β)が知られている．PPARはレチノイドX受容体(RXR)とヘテロ二量体を形成し，PPAR応答エレメントを介して，様々な遺伝子の転写調節に関与している．肝臓で主に発現しているPPARαは種々の脂肪酸により活性化されるので，血中遊離脂肪酸のセンサーとして働くという考え方がある．また，PPARαアゴニストには抗高脂血症治療薬fibratesが知られている．一方，PPARγは脂肪細胞やマクロファージで主に発現し，PPARγアゴニストとしてインスリン抵抗性改善薬rosiglitazoneなどのチアゾリジン誘導体，プロスタグランジン(PG)D_2の代謝産物15-deoxy-$\Delta^{12,14}$ PGJ_2などが知られている．PPARδは広く種々の細胞で発現し，その内因性リガンドとしてはプロスタサイクリンが候補となっているが，PPARはいずれも脂肪酸をリガンドとしている．最近，PPARδは脂肪燃焼の制御因子として，PPARγは脂肪貯蔵の制御因子として働くことが提唱されている．以上，PPARの3種類のサブタイプはそれぞれ異なった場所で異なった機能を発揮すると考えられるが，いずれも生活習慣病の標的分子として世界的に注目を集めている分子群である[4]．

我々はアスピリンなど非ステロイド性抗炎症薬の標的であるPG産生の律速酵素・誘導型シクロオキシゲナーゼ(COX-2)に関する研究を進めている．そしてグルココルチコイド受容体やPPARγなどの核内受容体がCOX-2の細胞特異的発現調節に関与することを報告した[5][6]．一方，表1に示すように発がんとPG，レスベラトロールの関わりについてはいくつかの報告がある．共同研究の結果，レスベラトロールががん細胞において，COX-2の活性および発現を抑制することを見いだした[10]．そこで種々の細胞でレスベラトロールの効果を検討した結果，COX-2の発現について細胞の種類によって異なっており，レスベラトロールがある種の核内受容体リガンドとして作用しているのではないかいう新しい

表1．発がんとプロスタグランジン，レスベラトロールの関わり．

1. 疫学的調査の結果，リウマチ患者などでアスピリンを長期間常用している患者は大腸がんによる死亡率が40～50％低い[7]．
2. 種々の化学発がん物質を用いたマウスでの発がん実験において，アスピリンなど非ステロイド性抗炎症薬(NSAIDs)は有意にがんの発生を抑制する．
3. ヒト家族性大腸腺腫症のモデルとなるマウスでの実験の結果，COX-2の活性を抑制すると，腺腫の大きさと数が有意に減少する[8]．
4. 赤ワインに含まれるレスベラトロールはマウス皮膚がんモデルで発がん抑制効果を示す[9]．

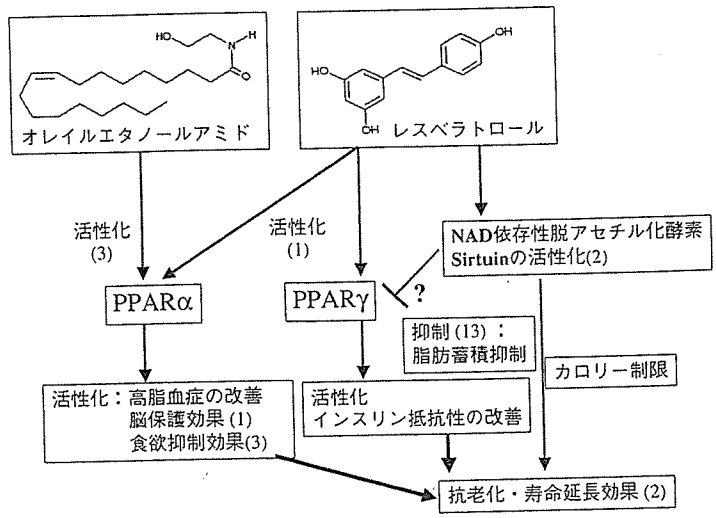

図1

着想を得た．そこで核内受容体の専門家である故梅園和彦博士(京都大学ウイルス研究所)，脳卒中の専門家である名村尚武博士(当時・国立循環器病センター，現クリーブランドクリニック)と共同研究を行い，1)レスベラトロールは核内受容体群のうち，PPARα およびPPARγを選択的に活性化する事，2)その活性化は血管内皮細胞およびニューロンで認められること，3)レスベラトロールおよびPPARα リガンドを3日間経口投与後に，24時間脳虚血にすると，脳梗塞の体積がコントロールに比べ有意に減少し，脳保護効果が認められること，4)その脳保護効果はPPARαノックアウトマウスでは認められないことを明らかにした．これらの結果から，レスベラトロールによるPPARα の活性化は，「フレンチパラドックス」を説明する新しい作用機構を提供し，PPARα が脳卒中に対する薬剤の新しい分子標的になることが示唆された[1]．現在，PPAR の活性化は脳保護効果以外にも生活習慣病に関連する種々の病態を改善することが報告されており，レスベラトロールの効果も広く生活習慣病予防に関与すると考えられる．しかし，その分子作用機構については不明な部分が多い．特に1)レスベラトロールの脳保護効果は1日の経口投与では認められず，3日以上の経口投与が必要であること，2)レスベラトロールによるPPAR の活性化能は肝臓よりも血管内皮細胞で強く，細胞選択性があることを見いだした．現在その分子機構について，PPAR 活性化の下流で働く分子群の同定とともに検討を行っている．

以前よりカロリー制限は，ラットで実験的に老化を遅らせ，寿命を延長させることが知られている[11]．そこでカロリー制限の機構を解明し，その効果のみを模倣する薬剤(カロリー制限模倣剤)の開発がおこなわれている．2003年にレスベラトロールがそのような作用を持ち，酵母の寿命をのばすことが報告された[2]．その効果はNAD^+ 依存性脱アセチル化酵素 Sirtuin ファミリーを活性化に由来すると報告されたが，Sirtuin はヒストンを介してさまざまな転写調節に関与しており，核内受容体とも相互作用していると考えられる．

もう一方で，オレイルエタノールアミド(OEA)は核受容体PPARα の活性化を介して食欲と体重をコントロールすることが報告された[3]．OEA は PPARα に高い親和性を持ち(EC_{50} = 10 nM)，その親和性はオレイン酸に対する親和性の1000倍と報告された．一方，OEA は PPARδ に対しても親和性をもつが(EC_{50} = 1.1 μM)，PPARγ には親和性を持たない．さらに，1) OEA は PPARα の活性化を介して，脂質代謝に関わるタンパク質の転写を高め，摂食刺激に関与する NO 合成酵素の誘導を抑制すること，2)自由に摂食させているマウスの小腸を時間差で調べると，えさを食べる夜間は OEA 濃度が低く，逆に満腹で休んでいる日中は OEA 濃度が高いことが報告され，OEA が PPARα の活性化を介して食欲

の調節をしていることが提唱された．なお，既にアラキドン酸のエタノールアミドであるアナンダミドはGタンパク質共役型受容体であるカンナビノイド受容体を介して，多幸感など，マリファナ様の作用を発揮することが知られている．それ故，オレイン酸のエタノールアミドであるOEAもカンナビノイド受容体に作用することも予想されたが，そのような作用は見いだされなかった．

これらの結果は我々が報告し，提唱しているPPARを介するレスベラトロールの生活習慣病予防と直接関連していると考えられる．図1にその概略を示す．最近，DNAチップによる解析で，カロリー制限を行ったネズミと核内受容体PPARαのアゴニストを投与したネズミではよく似た遺伝子の発現パターンを示し，寿命延長に関与するとの報告がなされたが[12]，これは我々の提唱するシナリオに合致している．しかし一方で，レスベラトロールで活性化されるSirtuinはPPARγの活性化を抑制することで白色脂肪細胞において脂肪代謝を活性化するという報告もなされた[13]．この結果は，レスベラトロールはPPARγも同時に活性化するという我々の報告とは一致しない．いずれにせよ，レスベラトロールと核内受容体の相互作用は，寿命延長，生活習慣病予防の視点から，今後さらに研究が進んでいくと考えられる．一方で，食品中の含まれるポリフェノール類と核内受容体の関係にも興味が持たれる．

(奈良女子大学生活環境学部　井上　裕康)

文　献

1) Inoue H, Jiang X, Katayama T, Osada S, Umesono K, Namura S (2003) Brain protection by resveratrol and fenofibrate against stroke requires PPARα in mice. *Neurosci Lett* **352**, 203-206
2) Howitz KT, Bitterman KJ, Cohen HY, Lamming DW, Lavu S, Wood JG, Zipkin RE, Chung P, Kisielewski A, Zhang LL, Scherer B, Sinclair DA (2003) Small molecule activators of sirtuins extend Saccharomyces cerevisiae lifespan. *Nature* **425**, 191-196
3) Fu J, Gaetani S, Oveisi F, Lo Verme J, Serrano A, Rodriguez De Fonseca F, Rosengarth A, Luecke H, Di Giacomo B, Tarzia G, Piomelli D (2003) Oleylethanolamide regulates feeding and body weight through activation of the nuclear receptor PPARα. *Nature* **425**, 90-93
4) Evans RM, Barish GD, Wang YX (2004) PPARs and the complex journey to obesity. *Nat Med* **10**, 355-361
5) Inoue H, Tanabe T, and Umesono K (2000) Feedback control of COX-2 expression through PPARγ. *J Biol Chem* **275**, 28028-28032
6) 井上裕康 (2003) 核内受容体PPARを介する誘導型シクロオキシゲナーゼの発現調節に関する研究．ビタミン **77**, 449-458
7) Giovannucci E, Egan KM, Hunter DJ, Stampfer MJ, Colditz GA, Willett WC, Speizer FE (1995) Aspirin and the risk of colorectal cancer in women. *N Engl J Med* **10**, 609-614
8) Oshima M, Dinchuk JE, Kargman SL, Oshima H, Hancock B, Kwong E, Trzaskos JM, Evans JF, Taketo MM (1996) Suppression of intestinal polyposis in Apc delta716 knockout mice by inhibition of cyclooxygenase 2. *Cell* **87**, 803-809
9) Jang M, Cai L, Udeani GO, Slowing KV, Thomas CF, Beecher CW, Fong HH, Farnsworth NR, Kinghorn AD, Mehta RG, Moon RC, Pezzuto JM (1997) Cancer chemopreventive activity of resveratrol, a natural product derived from grapes. *Science* **275**, 218-220
10) Subbaramaiah K, Chung WJ, Michaluart P, Telang N, Tanabe T, Inoue H, Jang M, Pezzuto JM, Dannenberg AJ (1998) Resveratrol inhibits cyclooxygenase-2 transcription and activity in phorbol ester-treated human mammary epithelial cells. *J Biol Chem* **273**, 21875-21882
11) McCay CM, Crowell MF, Maynard LA (1935) The effect of retarded growth upon length of lifespan and upon ultimate body size. *J Nutr* **10**, 63-79
12) Corton JC, Apte U, Anderson SP, Limaye P, Yoon L, Latendresse J, Dunn C, Everitt JI, Voss KA, Swanson C, Kimbrough C, Wong JS, Gill SS, Chandraratna R, Kwak M, Kensler TW, Stulnig TM, Knut R. Steffensen KR, Gustafsson J, Mehendale HM (2004) Mimetics of Caloric Restriction Include Agonists of Lipid-activated Nuclear Receptors. *J Biol Chem*, in press
13) Picard F, Kurtev M, Chung N, Topark-Ngarm A, Senawong T, Machado De Oliveira R, Leid M, McBurney MW, Guarente L (2004) Sirt1 promotes fat mobilization in white adipocytes by repressing PPAR-gamma. *Nature* **429**, 771-776

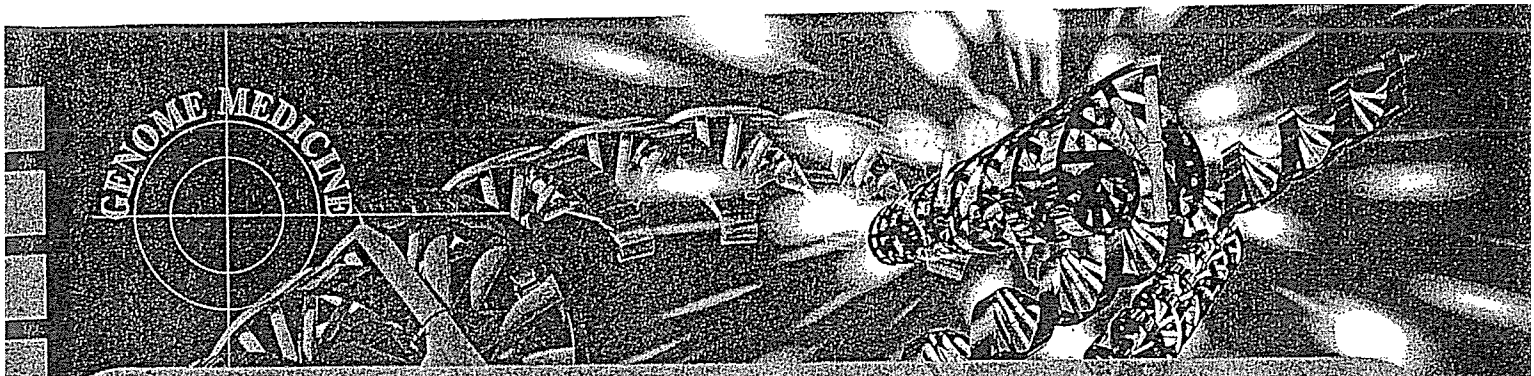

Ca^{2+}-permeableカチオンチャネルと筋変性

Ion channels and muscle degeneration

Key Words　⇒ゲノム用語解説105ページ～

⇒ジストロフィン(Dys)複合体
⇒細胞骨格系蛋白質
⇒心筋症
⇒ストレッチ感受性チャネル
(stretch-activated ion channel；SA-channel)
⇒TRPスーパーファミリー

岩田裕子[1]，片野坂友紀[1]
若林繁夫[1]，重川宗一[2]

1：国立循環器病センター研究所循環分子生理部
2：千里金蘭大学生活科学部生理学教授

はじめに

デュシェンヌ型筋ジストロフィー(DMD)の原因遺伝子は，1987年にジストロフィン(Dys)と確定されたが，筋ジストロフィーにおける筋細胞変性のくわしい分子メカニズムはいまだ明らかではない．表1は遺伝性筋ジストロフィー症の原因遺伝子をまとめたものである．これから，骨格筋筋細胞変性は，Dys複合体を含む細胞骨格系蛋白質の異常に起因する場合が多いことがわかる．興味深いことに，これらのうちいくつかのもの(色付きで示した)は，心筋異常，特に拡張型心筋症を引き起こすことが知られている．Dys複合体異常で起こる病態の場合，細胞膜を介するCa^{2+}流入の増大が筋細胞変性の引き金になることが強く示唆されおり，本稿では，このCa^{2+}流入チャネルについて最近の知見を述べる．

筋細胞変性の発症

DMD患者やDysを欠失する*mdx*マウスでは，クレアチンキナーゼ(CK)などの筋細胞質蛋白質の血液中への流出や細胞外に添加したEvans blueなどの膜非透過性色素の骨格筋細胞内への取り込みなどが観察され，これらは筋活動により増大することが以前から観察されてきた[1,2]．また，Dysを欠失する単離筋細胞やmyotubesは，低浸透圧ストレスに対して脆弱であることも報告されている[3]．Dys複合体は，筋細胞内のアクチン/コスタメア構造を細胞外マトリックスに連結し，細胞膜を機械的に安定化する役割を担っており，Dysの欠失は，筋細胞膜の機械的ストレスに対する脆弱性の原因になると考えられている．一方，Dys欠失筋細胞では，細胞内Ca^{2+}濃度異常が存在すると以前から指摘されている．これまでに，Ca^{2+}感受性蛍光色素を用いてDMD患者および*mdx*単離筋